Asian Journal of Chemistry; Vol. 27, No. 3 (2015), 907-918

ASIAN JOURNAL OF CHEMISTRY

http://dx.doi.org/10.14233/ajchem.2015.17412

Theoretical Study of Interatomic Properties of Ruthenium Half-Sandwich Anticancer Complexes Containing Ru-N Bonds

ADEBAYO A. ADENIYI and PETER A. AJIBADE*

Department of Chemistry, University of Fort Hare, Private Bag X1314, Alice 5700, South Africa

*Corresponding author: Fax: +27 86 5181225; Tel: +27 40 6022055; E-mail: pajibade@ufh.ac.za

Received: 18 February 2014; *Accepted*: 1 August 2014; *Published online*: 19 January 2015; AJC-16694

The intramolecular properties of five sets of ruthenium based anticancer complexes have been theoretically studied using DFT method. The results shows that these complexes are thermodynamically stable and the stability is significantly enhanced through the high level of polarizability (POL), charge transfer (CT) and electrostatic (ES) contributions which may contribute to their biological effects. The presence of carboxylic unit is found to enhance the contributions of these factors. The features of the QTAIM bond properties of the ruthenium-ligand bond shows they are non-covalent in nature and the bond properties are not significantly altered by the change in the chemical environment of the complexes from one type to the other. However, the QTAIM atomic properties of ruthenium changed significantly with the changes in the chemical environment of the complexes. The NEDA analysis shows that these types of complexes are predominantly characterized with ligand to metal charge transfer (LMCT).

Keywords: Ruthenium anticancer complexes, Polarizability, Stability, Intra and inter atomic properties.

INTRODUCTION

Several efforts have been made by the researchers at both computational and experimental levels to discover an alternative to *cis*-platin anticancer metal complex which still being used for more than 70 % of cancer cases[1,2]. Ruthenium based complexes seems to have attracted serious research attentions than any other metal complexes[3-10]. Even though there is yet to be any approved anticancer complexes that matches the anticancer activities of *cis*-platin, many of promising anticancer ruthenium complexes have been synthesized and analysed[11-16]. One of the leading organometallic complexes that have gain the serious research screening as anticancer complexes are the ruthenium half-sandwich complexes. Since the first synthetic route has been made known through the work of Bennett *et al.*[17-24] many of these complexes have been screened as anticancer[25-30].

In this study, five ruthenium half-sandwich complexes are selected for theoretical studies. These have the feature similar to the type of complexes that have gained researcher attention of the Sadler *et al.*[31-37] laboratory but a little defer because of the carboxylic and/or pyrazole unit (s) (Fig. 1) that are introduced into the complexes. Another notable anticancer complexes still at laboratory level are the RAPTA complexes from Dyson *et al.*[38-47] lab. These five complexes have been theoretically compare to the RAPTA complexes against many anticancer receptors and are predicted to be promising[48]. However, many of these complexes are known to have complicated chemistry and unstable[1]. Our efforts are directed toward understanding the chemistry of their stability in terms of their structural, conformational and electronic properties, intra and inter atomic properties, nature of the electron distribution which will enhance their rational design, development of their force fields and their biological activities. We are equally interested in discovering of more stable and biologically active ruthenium based complexes. Some of the significant properties of interest to us in this study is the non-covalent interactions that have been discovered to govern the stability of complexes[49]. Besides hydrogen bonds, the interactions between anions and π-systems have been pointed out to be among the strongest noncovalent interactions which depends on how electron-deficient is the π-system[49]. The theoretical methods have been used enough to complement and sometimes even to challenge experimental data in area like predict the geometries, vibrational frequencies, bond dissociation energies and other chemically important properties[50].

COMPUTATIONAL METHOD

The geometries of the complexes were optimized twice with PBE0 51 functional and a mixed basis sets SBKJC VDZ that have effective core potential (ESP)[52] approximation and

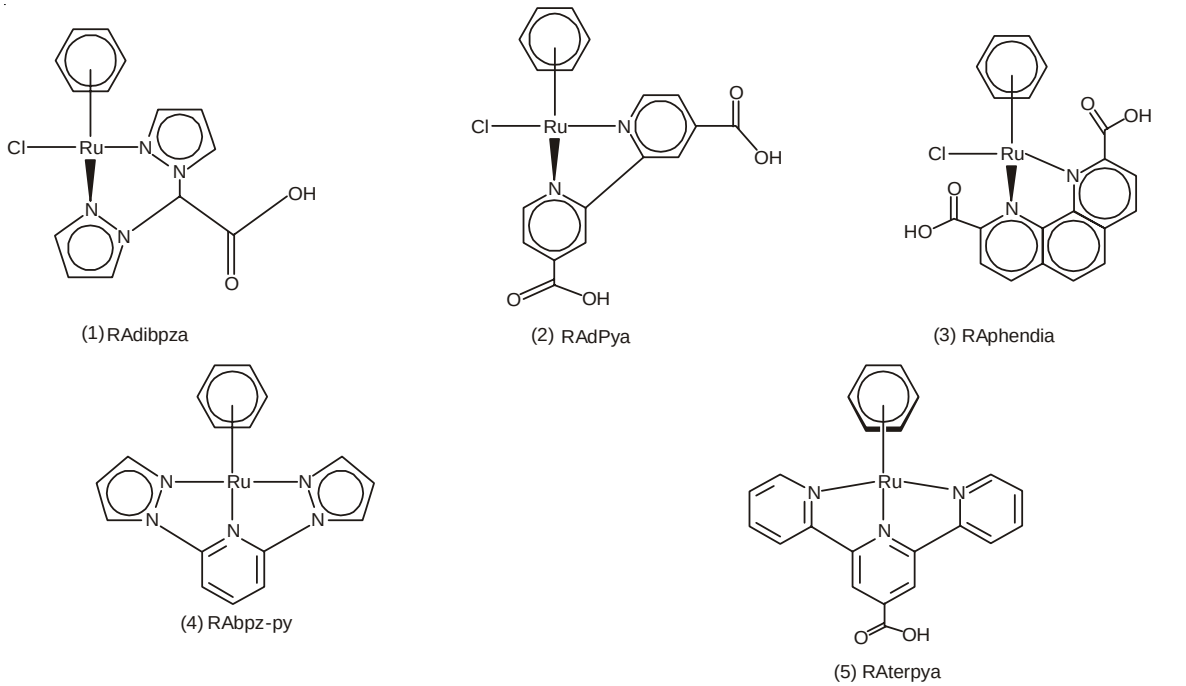

Fig. 1. Schematic structures of the five complexes

6-31G* or 6-31+G(d,p) basis set. In the first optimization, the ECP basis set SBKJC VDZ is applied on the Ru and Cl atoms where applicable while other atoms in the complexes are treated with basis set 6-31G* which shall subsequently be referred to as ECP(Ru,Cl)[6-31G*]. In the second optimization, the SBKJC VDZ is limited to only the ruthenium atom while the scaled up basis set 6-31+G(d,p) was applied on other atoms in the complexes which shall subsequently be referred to as ECP(Ru)[6-31+G(d,p)]. Other properties of the complexes are computed at B3LYP hybrid functional level of theories using other higher basis set like DGDVZP applied on Ru atom while other are treated with 6-31G* or 6-31+G(d,p) referred to as DGDVZP(Ru)[6-31G*] or DGDVZP(Ru)[6-31+G(d,p)]. Energy values of the systems are also estimated at a prohibitive MP2 method and at basis sets limit of aug-cc-pVTZ-DK and aug-cc-pVTZ applied on Ru and other atoms in the complexes, respectively referred to just as aug-cc-pVTZ subsequently. Many of the basis sets used for the computation are obtained from the external EMSL basis set library[53,54] and were incorporated into the two *ab-initio* packages[55,56], FIREFLY 08 and Gaussian 09 that were used for the computation in parallel processors. SBKJC VDZ ECP basis set with hybrid functional PBE0 has been shown to be effective in treating complexes with large number of electrons and has been applied in computing properties of many metal clusters[57,58] and also because ECP incorporate relativistic corrections for the metal atoms[59]. The Bader's quantum theory of atoms in a molecule (QTAIM) analysis were done mainly using the wavefunction obtained using B3LYP hybrid functional[60] and basis sets either ECP(Ru)[6-31+G(d,p)] or DGDVZP(Ru)[6-31+G(d,p)] or a minimal all electron basis[61] set 3-21G. A topological analysis was performed in order to calculate the charge density (r) and its second Laplacian derivative of charge density ($\Delta^2\rho$) for the bond critical points (BCP). AIMAll 12.06.03 package was used for QTAIM analysis[62] while the NBO 5.0G program[63] as implemented in FIREFLY 08 was used for the natural bond orbital (NBO) analysis[64] and natural energy decomposition analysis (NEDA)[65].

RESULTS AND DISCUSSION

The optimization and computation of the properties of these complexes were done twice, first applying ECP SBKJC VDZ basis set on Ru and Cl atoms where applicable and all other atoms treated with 6-31G* basis set while in the second method the ECP is limited to only the ruthenium atom and the other atoms in the systems are treated with 6-31+G(d,p) basis set which will subsequently be referred to as PBE0/ECP(Ru,Cl)[6-31G*] and PBE0/ECP(Ru)[6-31+G(d,p)], respectively. The hybrid functional PBE0 was used for the optimization while the properties were computed using another hybrid functional B3LYP. The ECP basis set SBKJC_VDZ combined with PBE0 has been known to give a good stationary geometries of metal complexes[57,58] and also because ECP incorporate relativistic corrections for the metal atoms[59]. Therefore, all the stationary geometries of the complexes studied are obtained using the PBE0/ECP(Ru,Cl)[6-31G*] and PBE0/ECP(Ru)[6-31+G(d,p)] and the respective thermodynamic properties obtained from these are show in Table-1. Change of the functional significantly affects the total energy of these complexes than changes in the basis sets (Table-2). The functional B3LYP in all the cases over estimate the energy of the system while PBE0 gives values closed to higher perturbation method of MP2 as show in Table-2. This further support the literature reports that metal complexes is better optimized using PBE0 with ECP basis sets[57,58]. However, the NBO, NEDA and QTAIM properties of the complexes are computed using B3LYP functional because

it is one of the most used functional in computational studies and also shown to behave well in computing QTAIM properties[66]. Considering the functional B3LYP only, there is a very closed relationship in the energy values computed by scaling up the basis set to a limit of aug-cc-pVTZ-DK as shown in Table-2. The energies are computed following the scaling: 3-21G → ECP(Ru,Cl)[6-31G*] → ECP(Ru)[6-31+G(d,p)] → DGDZVP(Ru)[6-31G*] → DGDZVP(Ru)[6-31+G(d,p)] → aug-cc-pVTZ-DK. The basis set aug-cc-pVTZ-DK and the functional MP2 are prohibitively expensive for computing the properties of these type of metal complexes with atoms ranging from 36-45, therefore the energy values provided for functional MP2 and basis set aug-cc-pVTZ-DK in Table-2 are the unconverged values. The QTAIM properties of the complexes are computed using 3-21G, DGDZVP(Ru)[6-31+G(d,p)] and ECP(Ru)[6-31+G(d,p)] basis sets but the NBO and NEDA analysis a limited to only the higher combination of basis set DGDZVP(Ru)[6-31+G(d,p)]. In line with the literature reports, we observed that all methods could either overestimate or underestimate QTAIM properties (Table-8)[66].

The interest of this work is to understand the chemistry of these five Ru(II)-based anticancer complexes based on their intramolecular interactions, strength of the Ru-N bonds and the stability of these complexes in relation to their proposed anticancer behaviours[48].

Thermodynamic and the geometry properties: The schematic geometries of the five complexes studied in this work are shown in Fig. 1. These are half-sandwich complexes with bidentate (complexes 1, 2 and 3) and tridentate (complexes 4 and 5) ligands. Both complexes 4 and 5 have no chloride atom as ligand and there is no carboxylic unit in complex 4 among all other complexes. The high negative values of the energy, enthalpy and the free energy of the complexes at both levels of theories (Table-1) show that they are thermodynamically stable complexes. The values of the thermodynamic properties of the complexes at the two levels of theories ECP(Ru,Cl)[6-31G*] and ECP(Ru)[6-31+G(d,p)] as applied for their optimization are shown in Table-1. The properties of complexes 4 and 5 that have no chloride atoms shows that increasing the basis set do not have any serious effect on the thermodynamic properties of the complexes. But when the chloride atom(s) in complexes 1, 2 and 3 are treated with all electron basis 6-31+G(d,p) instead of ECP basis set SBKJC VDZ, there is a change in the thermodynamic properties except for the entropy (S), heat capacity (CV) and thermal correction to the energy (TCE). Also, the geometry of complex 4 was predicted as transition in PBE0/ECP(Ru,Cl)[6-31G*] but found to be stable in a higher basis set PBE0/ECP(Ru)[6-31+G(d,p)].

All the present metal-ligand bonds in the complexes with their bond order obtained through NBO analysis are shown in Table-3. The ruthenium-nitrogen (Ru-N) bonds are the shortest bonds in all the complexes ranges from 2 to 2.162 while their bond orders ranges from 0.361 to 0.424, which are relatively within the bond order of Ru-C_{arene} bonds. Comparing to the available experimental Ru-N bond lengths, the computed Ru-N_{bpyr} bonds in complex 2 (where subscript bpyr indicates ruthenium-bipyridine bonds) are both 2.09 Å while R-N_{phn} in complex 3 (where subscript phn indicates ruthenium-phenanthroline bonds) are both 2.138 Å which are closed to the experimental range of values for Ru-N_{bpyr} (2.040 to 2.056 Å) and for R-N_{phn} (2.073 to 2.087 Å) bonds[67]. In a good agreement with the experimental reports typical of Ru-N_{bpyr} and R-N_{phn}, the Ru-N_{bpyr} bonds in complex 2 is shorter than the R-N_{phn} bonds in complex 3. The bond order (Table-3) with the

TABLE-1
THERMODYNAMIC PROPERTIES OF THE COMPLEXES IN KJ/Mol or KJ/Mol-K

Complexs	E0	E	H	G	TC E KJ/mol	CV KJ/Mol-K	S KJ/Mol-K	Imaginary	No. nor vib mode
PBE0/ECP(Ru,Cl)[6-31G*]									
1	-2.67E+06	-2.67E+06	-2.67E+06	-2.67E+06	7.51E+02	0.32	0.62	0	102
2	-3.18E+06	-3.18E+06	-3.18E+06	-3.18E+06	8.15E+02	0.37	0.69	0	114
3	-3.38E+06	-3.38E+06	-3.38E+06	-3.38E+06	8.48E+02	0.39	0.69	0	120
4	-2.68E+06	-2.68E+06	-2.68E+06	-2.69E+06	8.08E+02	0.31	0.55	1	108
5	-3.30E+06	-3.30E+06	-3.30E+06	-3.30E+06	9.52E+02	0.38	0.66	0	129
PBE0/ECP(Ru)[6-31+G(d,p)]									
1	-3.84E+06	-3.84E+06	-3.84E+06	-3.84E+06	7.49E+02	0.32	0.62	0	102
2	-4.35E+06	-4.35E+06	-4.35E+06	-4.35E+06	8.13E+02	0.37	0.69	0	114
3	-4.55E+06	-4.55E+06	-4.55E+06	-4.55E+06	8.46E+02	0.70	0.39	0	120
4	-2.69E+06	-2.68E+06	-2.68E+06	-2.69E+06	8.06E+02	0.31	0.55	0	108
5	-3.30E+06	-3.30E+06	-3.30E+06	-3.30E+06	9.49E+02	0.38	0.66	0	129

TABLE-2
TOTAL ENERGY OF THE COMPLEXES IN KJ/Mol COMPUTED SCALING UP THE FUNCTIONAL AND BASIS SETS

Functional/basis sets	1	2	3	4	5
PBE0/ECP(Ru,Cl)[6-31G*]	-2.6733E+06	-3.1824E+06	-3.3823E+06	-2.6853E+06	-3.2957E+06
B3LYP/3-21G	-1.5195E+07	-1.5700E+07	-1.5899E+07	-1.4042E+07	-1.4649E+07
PBE0/ECP(Ru)[6-31+G(d,p)]	-3.8441E+06	-4.3515E+06	-4.5514E+06	-2.6858E+06	-3.2962E+06
B3LYP/ECP(Ru)[6-31+G(d,p)]	-1.5265E+07	-1.5773E+07	-1.5973E+07	-1.4107E+07	-1.4718E+07
MP2/ECP(Ru)[6-31+G(d,p)]	-3.8288E+06	-4.3340E+06	-4.5329E+06	-2.6712E+06	-3.2789E+06
B3LYP/DGDZVP(Ru)[6-31G*]	-1.5266E+07	-1.5774E+07	-1.5974E+07	-1.4108E+07	-1.4719E+07
B3LYP/DGDZVP(Ru)[6-31+G(d,p)]	-1.5265E+07	-1.5773E+07	-1.5973E+07	-1.4107E+07	-1.4718E+07
B3LYP/acc-pvtz	-1.5069E+07	-1.5576E+07	-1.5773E+07	-1.3907E+07	-1.4520E+07
SCF of the both MP2/DGDZVP(Ru)[6-31+G(d,p) and B3LYP/aug-cc-pVTZ are prohibitively expensive and therefore is unconverged					

TABLE-3
BOND DISTANCES (Å) AND BOND ORDER OF THE RUTHENIUM LIGAND BONDS OF THE COMPLEXES

bpyr			dpy			pth			raz			ter		
Pair	Dist	Order	Pair	Dist	Order	Pair	Dist	Order	Pair	Distance	Order	Pair	Dist	Order
Ru-C9	2.267	0.387	Ru-C7	2.233	0.408	Ru-C13	2.236	0.376	Ru-C2	2.262	0.384	Ru-C20	2.269	0.399
Ru-C13	2.232	0.428	Ru-C8	2.254	0.371	Ru-C18	2.236	0.375	Ru-C5	2.241	0.435	Ru-C23	2.290	0.361
Ru-C18	2.236	0.401	Ru-C13	2.277	0.350	Ru-C25	2.261	0.414	Ru-C3	2.252	0.413	Ru-C26	2.269	0.399
Ru-C10	2.226	0.414	Ru-C18	2.233	0.408	Ru-C14	2.251	0.390	Ru-C6	2.252	0.412	Ru-C18	2.252	0.419
Ru-C16	2.228	0.405	Ru-C14	2.239	0.360	Ru-C21	2.264	0.411	Ru-C4	2.263	0.384	Ru-C22	2.252	0.419
Ru-C19	2.222	0.378	Ru-C19	2.254	0.372	Ru-C23	2.253	0.387	Ru-C7	2.242	0.435	Ru-C27	2.289	0.361
Ru-Cl22	2.394	1.007	Ru-Cl10	2.396	1.052	Ru-Cl7	2.390	0.996	Ru-N10	2.162	0.363	Ru-N14	2.152	0.423
Ru-N12	2.137	0.361	Ru-N11	2.096	0.431	Ru-N10	2.138	0.371	Ru-N13	2.162	0.363	Ru-N15	2.039	0.470
Ru-N17	2.139	0.361	Ru-N16	2.096	0.430	Ru-N16	2.138	0.371	Ru-N15	2.084	0.417	Ru-N21	2.153	0.424

Laplacian values ($\nabla^2\rho(r)$) of the electron density of the bonds (Table-8) also indicate that the Ru-N_{bpyr} is stronger than the R-N_{phn} in perfect agreement with the experimental report[67]. Considering the one N-Ru-N angle in complexes 1 to 3 and the three N-Ru-N angles 4 to 5, the optimized geometries have 82.81, 77.12, 77.32, 107.85 (52.58, 72.18), 108.69 (51.90, 73.67) for complexes 1, 2, 3, 4 and 5, respectively. The computed N-Ru-N angle of complex 2 is a little lower than complex 3 which agrees with the experimental order and range of values 78.9 and 79.5 to 80.1 typical of N_{bpyr}-Ru-N_{bpyr} and N_{phn}-Ru-N_{phn}, respectively[67]. The Ru-C_{arene} bonds ranges from 2.222 (in complex 1) to 2.289 Å (in complex 5) and their bond orders ranges from 0.35 (in complex 2) to 0.435 (in complex 4). The Ru-Cl bonds distances range from 2.39 to 2.396 and their bond order ranges from 0.996 to 1.052. Both the computed Ru-C_{arene} and Ru-Cl bonds are within the experimental ranges of 2.197 to 2.257 Å for Ru-C_{arene} and 2.410 to 2.434 for Ru-Cl as reported for RAPTA complexes[68]. The features of bond orders suggest Ru-Cl to be strongest (Table-3) but disapproved from the QTAIM analysis (Table-8) which shows it is weaker than other bonds and will be a good leaving unit for the activation of these complexes by hydrolysis[41,69,70].

The HOMO of the complexes is predominantly the metal atom and the chloride atom where applicable which indicate the electrons being pulled away from metal orbital by the coordinated ligand and also electron being back-bonded into the metal's low lying orbital from the coordinated ligand atoms which responsible for the metal atom being also part of the LUMO. A clear picture of these electron withdrawing and charge transfer is presented in the NBO and NEDA analysis of the complexes. The nature of the LUMO shows that the arene group and other ligands draw electron from the metal during coordination and also there is back bonding of electrons into the vacant lower anti-bonding lone pair orbitals of metal atom. The bipyridine (bpyr) and the phenanthroline (phn) units dominates the LUMO of complexes 2 and 3, respectively which shows they are more electron withdrawing than the *bis*-(pyrazol-1-ly)methane ligand of complex 1. Also, the central pyridine unit of the *bis*-(pyrazol-1-ly)pyridine and terpyridine of complexes 4 and 5 equally dominate the LUMO part of the complexes Fig. 2.

Features of H-bonding and Ru-N bonds: Hydrogen bond is the most widely studied noncovalent interaction in chemical and biological systems because of its significance important to the stability, biological functions of compounds[71-74]. It is reported to be undoubtedly the most important weak interaction in nature[73]. To the best of our understanding, this is the first time the intramolecular H-bonding of these type of the complexes are reported (Table-4). In complex 1, there are two H-bonds between the carbonyl oxygen atom of carboxylic and the two adjacent H atoms of the pyrazole units. The classical understanding is that there should be elongation of the two C-H that are involved in the H-bonding and consequentially lead to the weakening of the bonds[71]. This classical effect is observed in complex 1 as the C5-H24 and C15-H29

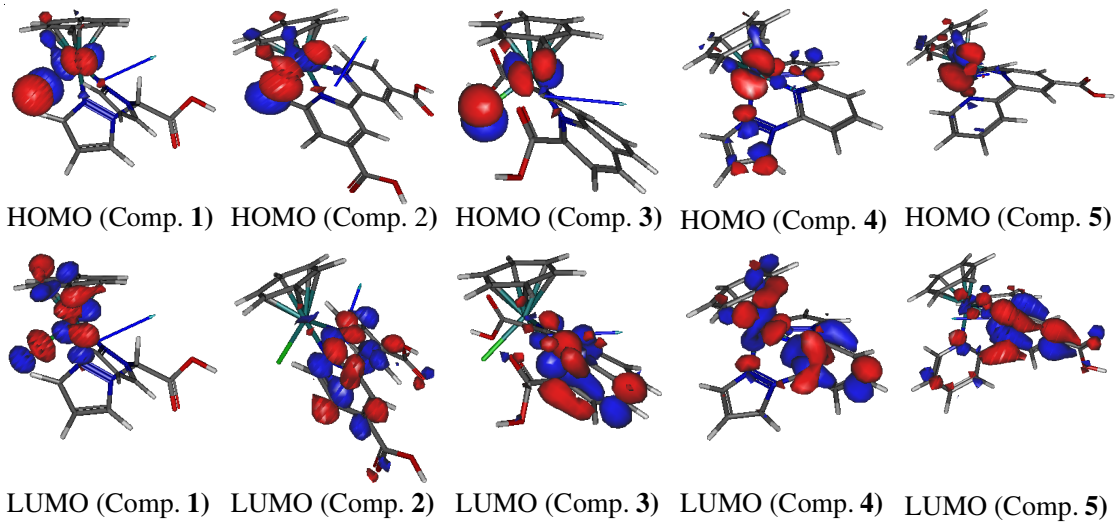

Fig. 2. HOMO and the LUMO of the complexes

TABLE-4
H-BONDING PROPERTIES OF THE COMPLEXES

	ρ(r)	$\nabla^2\rho(r)$	Ellipticity	K	BPL -GBL_I	V	G	L	GBL_I	V/G
Complex 1										
O2···H24	0.0101	0.0388	0.4777	-0.0016	0.1887	-0.0065	0.0081	-0.0097	4.7207	0.7994
O2···H29	0.0100	0.0384	0.5142	-0.0016	0.1942	-0.0064	0.0080	-0.0096	4.7341	0.7961
					0.0000					
H34···H38	0.0092	0.0403	1.7449	-0.0027	0.5505	-0.0047	0.0074	-0.0101	4.0818	0.6359
					0.0000					
O2···H31	0.0164	0.0614	0.3859	-0.0018	0.1265	-0.0118	0.0136	-0.0154	4.2711	0.8686
O28···H36	0.0168	0.0625	0.3248	-0.0017	0.1049	-0.0122	0.0139	-0.0156	4.2285	0.8778

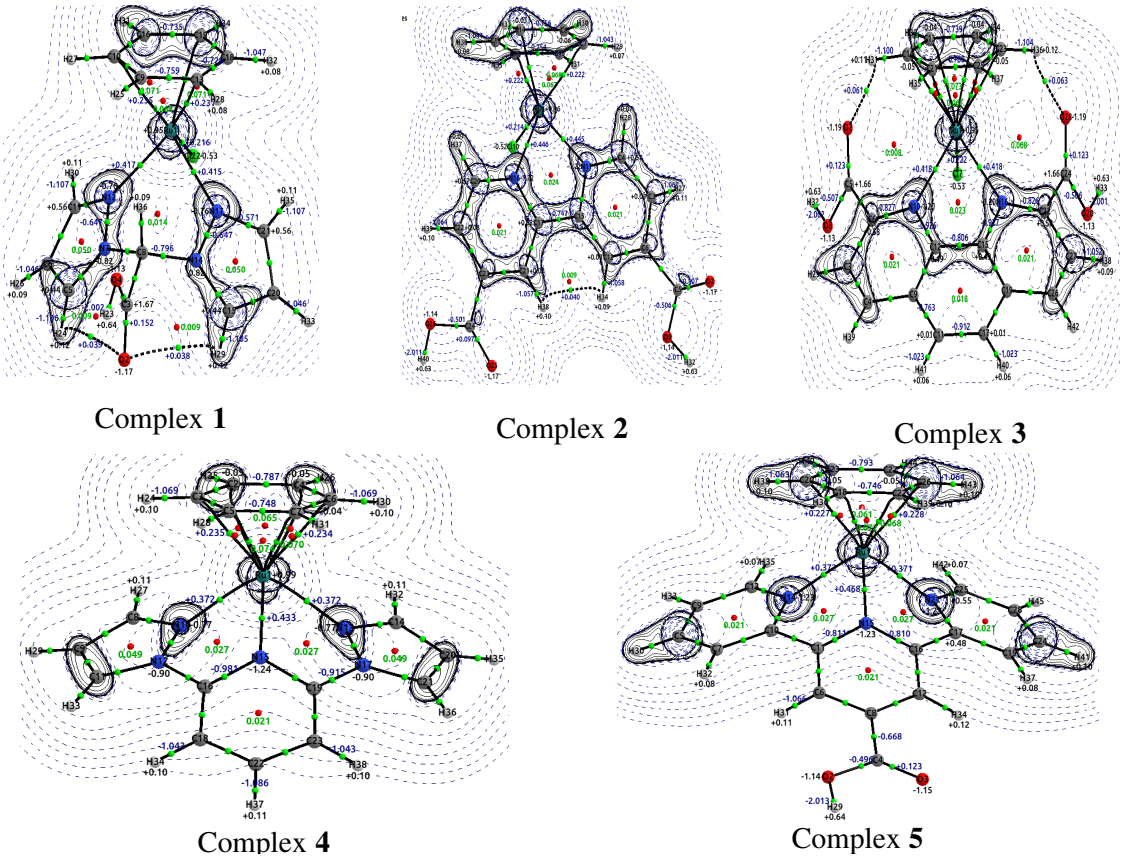

Fig. 3. Laplacian of the electron density plots in the plane of N, Ru and N nuclei (positive contours as solid and negative contours as dashes lines are drawn from 0 to ±800) showing the features of bonds (strong bonds in solid and hydrogen bond in dash lines) for five complexes

that are involved in H-bonding are weaker with Laplacian ($\nabla^2\rho(r)$) of -1.106 and -1.105 compare to C11-H30 and C21-H35 with $\nabla^2\rho(r)$ of -1.107 and -1.107, respectively which are in the same ligand chemical environment (Fig. 3). The bond length of the two C-H bonds that are involved in H-bonding also are found to increase and consequentially have higher bond extension than the rest of the C-H bonds. The higher H-bonding of the H24···O2 than the H29···O2 is reflected in their receptive C-H has that of the formal is shorter than the later. The H atoms that are involved in the H-bonding become more electropositive while the C atoms of the C-H bonds becomes less electropositive compare to carbon in the same chemical environment (Fig. 3). An additional two rings are added as a result of the H-bonding but have the lowest electron density (0.009) while the ring form by the Ru and the arene C atoms have the highest electron density (0.068 to 0.071) which is a clear indication that electrons are directed towards the π-arene ligands from the metal. Also, in all the complexes, the arene-Ru ring has the highest electron density compare to other rings in each of the complex. The C=O unit of the carboxylic in complexes 1 and 3 contributes significantly to the H-bonding networks of the complexes and the total hydrogen stability energy of the complexes 1, 2, 3 and 5 with carboxylic unit (Table-7). There is every possibility that the near contact effect of the two carboxylic units contribute to the observed H···H hydrogen bond observed in complex 2. This type of interaction is not completely strange as it was observed in the H2-HH non-covalent interaction[72,73]. This unusual H···H interaction gives the bipyridine in complex 2 a feature that looks like a pseudo phenanthroline as in complex 3. This could also be

one of the reasons why during our previous theoretical docking, these two complexes are found similar in their receptor binding which resulted to the two complexes frequently rated high in many cases[48]. These complexes have the highest stabilization energy which are in a closed range compare to other complexes.

Considering the strength of the H-bonds formed (the $\nabla^2\rho(r)$ in bracket) in complexes 1 (+0.038 and +0.039), 2 (+.040) and 3 (+0.061 and +0.063), the strongest one is in complex 3 while that of complex 1 is the lowest (Table-4). The H···H interaction in complex 2 has greater ellipticity and bond stretching than other H-bonds in other complexes yet its strength is still a bit higher than H-bonds in complex 1 considering their $\nabla^2\rho(r)$ values (Table-4). Though the H-bonding of H···H in complex 2 has the smallest s electron density at the bcp, yet the value is a clear indication that it is not a van der Waals interaction since it lies within the range of proposed for H-bonding interactions[73]. The ring electron density form by the H-bonding in complex 3 (0.008) is the lowest compare to other rings form from the H-bonding in other complexes which may be traced to the effect of its seven member rings compare to others that are six member rings. Another interesting features of the C-H that acts as proton donor in complexes 1 and 2 is that its C atom becomes less electropositive and its electronic volume appreciate while proton becomes more electropositive and its electron volume depreciate when compare to another C-H in the same chemical environment. This further indicates the elongation and weakening of the C-H bonds as a result of the H-bonding. The feature of the proton donor C-H bonds, which are part of the arene as in complex 3, is a bit different from what was observed in complexes 1 and 2. Though the H atom involved in H-bonding appreciate in electropositivity, the electropositivity of C atom of the proton donors C-H still falls within the range of values of other C atoms of the arene. Also, the strength of the proton donor C-H bond increases contrary to what was observed in complex 1 and 2. This further give another feature of H-bonding, which is contrary to the conventional features, as also reported in the literatures[71].

In complex 1, the electronic density of the RCP of the ligand with the Ru atom (0.014) is lower that the two normal RCP within the ligand itself (0.050), which is an indication of stronger, ring within the ligand but weaker ring with the Ru atom. The reverse is the case in complex 2, which is responsible for stronger Ru-N bonds in complex 2 ($\nabla^2\rho$ + 0.446 and +0.445) compare to complex 1 ($\nabla^2\rho$ + 0.417 and +0.415). The strength of the Ru-N also follow the same trend in complex 3 where the ring formed by the phenanthroline with Ru (0.023) is stronger that other three rings form within the ligand itself resulting to stronger Ru-N bond ($\nabla^2\rho$ + 0.418) than complex 1 but less than complex 2. The strength of the three Ru-N bonds in complex 4 varies with that of the mid pyridine unit of the tridentate ligand having the highest strength ($\nabla^2\rho$ + 0.433) while that of the two pyrazole units have lower strength (Lap + 0.372). Just as was observed in complex 1, the pyrazole rings have higher electron density that the rings formed with the Ru atom while that of the pyridine unit likewise follows the nature of lower ring electron density as in complex 2. In complex 5, the electron density of the rings within the tridentate ligands are lower than the two formed with Ru atom. Just as was observed in complex 4, the mid Ru-N bond (+0.468) is stronger than the other two Ru-N bonds (Lap + 0.372 and +0.371). The two outer Ru-N bonds in complexes 4 and 5 are relatively the same despite the changing from the pyrazole units to pyridine units. The strength of the ring electron density depends mostly on the number of the atoms that form the rings as higher number of atoms involve in ring formation results in lower ring electron density. In all the complexes, the strength of the Ru-N bonds is higher than the Ru-C bonds and Ru-Cl bonds in the complexes. Considering the mid Ru-N bonds in complexes 4 and 5, the order of the Ru-N bonds in the five complexes is 5 > 2 > 4 > 3 > 1 which agrees with the experimental report of stronger Ru-N_{bpyr} bonds than[67] Ru-N_{phn}.

Nature of the charge transfer and stability of the complexes: The NBO analysis further gives insight into the factors that determine the stability of the complexes. In all the complexes, the percentages of Lewis orbital (96.92, 96.30, 96.56, 96.77 and 96.28 % for complexes 1, 2, 3, 4 and 5 respectively) is far higher that the non-Lewis orbitals valence (2.90, 3.52, 3.25, 3.05 and 3.53 %) and non-Lewis Rydberg (0.19, 0.19, 0.19, 0.18 and 0.19 %). The lowest percentages of non-Lewis Rydberg and highest percentages of Lewis orbital indicate that geometry is stable. Also, relatively significant percentages of the Valence non-Lewis orbitals shows the important of charge transfer which can be metal to ligand (MLCT) or ligand to metal (LMCT) in determination of the stability of the complexes. The donor and the acceptors NBO that have the perturbation stabilization energy ($E^{(2)}$) ≥ 10 kcal/mol are presented and the amount of the electron (e) transferred into the anti-Lewis orbitals of the acceptors are presented in Table-5. The features of the perturbation energy show that they are dominated with back bonding of electrons from the lone pair of the ligand atoms to the anti-Lewis lone pair (LP) orbitals of the Ru atom. This characteristic feature of LMCT is an indication that during bonding there have been huge transfers of electron from metal to the ligands which are then compensated for with back-bonding of electron into the low lying lone pair (anti-Lewis orbitals) of the metal. In complexes 2 and 3 there is transfer of electrons from the ruthenium metal into the Lewis lone pair orbital of nitrogen atom of ligands. Also, there is charge transfer from metal lone pair into the C=C bond of the arene which is responsible for the little feature of MLCT. The amount of electrons that were transferred into all the anti-Lewis orbitals (acceptors) with the energy level of the orbitals is shown in Table-5. There is a significantly high amount of electron transfer into the anti-Lewis lone pair orbitals of metal atom. The NEDA analysis gives us a better understanding of the features of LMCT and MLCT of the complexes. From the NEDA, it is observed that the features of LMCT overshadowed the presence of MLCT. The lone pairs in the metal atom (both Lewis and non-Lewis) are the main orbitals that are involve in the charge transfer. When the total number of charges that were transferred from the metal atom in each complexes (0.27124, 0.32847, 0.26822, 0.31678 and 0.34006 for complexes 1, 2, 3, 4 and 5, respectively) are subtracted from the amount accepted from the ligands (1.45466, 1.50565, 1.47907, 1.42732 and 1.451 for the respective complexes), then a total of 1.21085, 1.17718, 1.18342, 1.11054 and 1.11094 charges were transferred from the ligands to metal central atom indicating that these complexes are characterized with LMCT.

TABLE-5
AMOUNT OF ELECTRON TRANSFERRED TO THE ACCEPTOR ORBITALS ND THEIR ENERGY LEVEL VALUES FOR THE FIVE COMPLEXES

1				2				3				4				5			
Obt	Acceptor	e	Energy	Obt	Acceptor	e	Energy	Obt	Acceptor	e	Energy	Obt	Acceptor	e	Energy	Obt	Acceptor	e	Energy
102	n*(4)Ru	0.87434	0.35967	115	n*(4)Ru	0.87533	0.35947	121	n*(4)Ru	0.86496	0.34522	98	n*(4)Ru	0.76334	0.4648	115	n*(4)Ru	0.77615	0.45347
103	n*(5)Ru	0.74736	0.33432	116	n*(5)Ru	0.75181	0.33217	122	n*(5)Ru	0.74216	0.31543	99	n*(5)Ru	0.75292	0.46237	116	n*(5)Ru	0.77258	0.45078
104	n*(6)Ru	0.21177	0.01293	117	n*(6)Ru	0.21035	0.01637	123	n*(6)Ru	0.20406	0.02081	100	n*(6)Ru	0.18956	0.12562	117	n*(6)Ru	0.18824	0.11449
403	σ*(2)C9C13	0.36325	0.14514	456	σ*(2) C7C13	0.39975	0.14684	488	σ*(2)C13C14	0.32278	0.10755	398	σ*(2)C2C4	0.30837	0.25545	114	n(2) N 21	1.31156	0.47767
406	σ*(2)C10C16	0.35698	0.13511	459	σ*(2) C8C14	0.38484	0.13694	500	σ*(2)C18C23	0.32044	0.10717	401	σ*(2)C3C5	0.31954	0.25861	507	*(2)C18C20	0.31805	0.24868
423	σ*(2)C18C19	0.33342	0.13002	475	σ*(2)C18C19	0.41816	0.14586	506	σ*(2)C21C25	0.34831	0.12365	408	σ*(2)C6C7	0.31948	0.25857	516	*(2)C22C26	0.31775	0.24853
																519	σ*(2)C23C27	0.30475	0.24754

The fragmentation of the complexes into different units (Table-6) gives the features of the synergistic effect of the metal coordinated fragments on each other. The induced energy is derived from the difference between the localized energy ΨA (def) and optimized energy ΨA (cp). Also, the induce dipole is from the difference between the dipole moment for the perturbed (def) and optimized (cp) wavefunction which can be interpreted as each unit in isolation and in the presence of each other, respectively. It is observed that the stability of the ligand units of these complexes were strongly enhanced through the synergistic effects where the bidentate unit in complexes 1, 2 and 3 and tridentate unit of complexes 4 and 5 (fragment unit two in all the complexes) are the most enhanced. The next to this is the arene unit (fragment unit three in complexes 1, 2 and 5, fragment unit four and two in complexes 3 and 4, respectively) which is also characterized with lower energy minimum. The improved dipole moment of the charge donor (predominantly the ligands) than the charge acceptor (predominantly metal centre *i.e*., fragment unit one) is an indication that the ligand fragments are characterized by significant polarization and thereby better exposing them as donor to the electrophilic attack than how the metal centre (acceptor) is exposed to nucleophilic attack. This suggest the possible reason while our docking results of these complexes indicates that the metal centre will hold the ligands preferentially in better position for receptor interaction than participating in residue interactions.

TABLE-6
INDUCED ENERGY AND DIPOLE OF EACH FRAGMENT OF LIGANDS COORDINATED TO METAL THROUGH NEDA ANALYSIS FOR THE FIVE COMPLEXES

Compl.		Fragment 1	Fragment 2	Fragment 3	Fragment 4
1	E(ind)	-0.8162	-1.7613	-1.5040	-0.7680
	Dipole (ind)	0.3878	7.4842	1.1558	1.0618
2	E(ind)	-0.8371	-2.0440	-1.4205	-0.7389
	Dipole (ind)	0.3398	5.0347	1.0371	1.0819
3	E(ind)	-0.8263	2.1367	-0.7788	-1.4994
	Dipole (ind)	0.4199	11.5244	1.0331	1.3137
4	E(ind)	-0.8337	-1.2962	-1.7371	–
	Dipole (ind)	0.3263	1.1486	6.7520	–
5	E(ind)	-0.8695	-2.2202	-1.3309	–
	Dipole (ind)	0.3455	6.2617	1.2446	–

It is obvious from the features of the NEDA analysis (Table-7) that the polarizability (POL) is the predominant factor that determines the stability of these complexes except in complex 2 where charge transfer (CT) is a little prevalent than polarizability. Electrostatic energy (ES) also contribute significantly to the stability of the complexes after the effects of the polarizability and charge transfer. It is the combined effects of polarizability, charge transfer and electrostatic that eventually help in overcoming the high core electron repulsion energy (XC+DEF-SE) and determines the high stability defined as total hydrogen energy of interaction (E) (Table-7). Complexes 2 and 3 are significantly stable than the rest of the complexes and complex 4. However, the main reason for the lower stability energy of complex 4 can be traced to the low magnitude of charge transfer due to the absence of carboxylic unit in the complex compare to other complexes. The presence of higher number of carboxylic unit in complexes 2 and 3 (two in each) should be responsible for higher charge transfer and electrostatic which consequentially resulted to higher stability energy of these complexes above others but the values of the polarizability does not follow the trend. The stability contribution of carboxylic unit in these complexes and the possibility of this carboxylic unit taking part in the biological interactions could be responsible for the theoretically proposed higher anticancer activities of these complexes[48].

Bond properties from QTAIM analysis: The bond properties of the complexes are computed through QTAIM analysis using AIMAll package. For the systems optimized with PBE0/ECP(Ru,Cl)[6-31G*], the properties were computed using functional with all electron minimal basis set B3LYP/3-21G while the properties of the systems that were optimized

TABLE-7
NEDA ANALYSIS OF THE COMPLEXES SHOWING THE CONTRIBUTION OF DIFFERENT FACTORS TO THE TOTAL INTERACTION ENERGIES (*i.e*., STABILITY ENERGIES)

	1	2	3	4	5
SE	818.92	760	835.99	747.73	794.78
ES	-825.88	-1121.16	-1087.51	-362.65	-589.75
POL	-1630.15	-1513.15	-1666.82	-1490.34	-1582.56
XC	-316.08	-307.19	-324.34	-272.18	-285.7
Electrical (Elec= ES+POL+SE)	-1637.11	-1874.31	-1918.35	-1105.26	-1377.52
Charge Transfer (CT)	-1197.82	-1566.92	-1559.06	-721.95	-1107.53
Core (XC+DEF-SE)	1908.05	2095.8	2128.62	1406.67	1693.56
Total Interaction (E=Elec + CT + Core)	-926.89	-1345.43	-1348.79	-420.55	-791.49

Components of energy are defines in terms of electrostatic interaction (ES); polarization (POL); electrical self-energy (SE); exchange interaction (XC); deformation energy (DEF), Electrical (ES+POL+SE), Core (XC+DEF-SE) and Total Interaction energy which is the final net H-bond energy (E = Electrical + Core + CT)

with PBE0/ECP(Ru)[6-31+G(d,p)] were computed using both the PBE0/ECP(Ru)[6-31+G(d,p)] and B3LYP/DGDZVP(Ru)[6-31+G(d,p)] functional and basis sets. The bonds properties are presented for the B3LYP/DGDZVP(Ru)[6-31+G(d,p)] in Table-8, for B3LYP/3-21G and PBE0/ECP(Ru)[6-31+G(d,p)]. The feature of Laplacian plots of electron density for all the complexes using B3LYP/DGDZVP(Ru)[6-31+G(d,p)] basis sets is shown in Fig. 3. In the correlation among the computed bonds properties (for B3LYP/DGDZVP(Ru)[-31+G(d,p)] only), the first thing that was observed is the disappearance of the NNCP in the topological surface of these complexes when the ECP basis set is limited to only ruthenium atom but appears especially in complexes 1, 2 and 3 when the chloride atom was also treated with ECP as explained for the optimization. The features of NNCP in molecules have attracted different controversial explanations[75-77] but in our complexes, it only exists when the ECP could not accurately approximate the core electrons of atoms other than metal in the construction of the molecular topologies. This agree well with the reason that the NNCP originate from the shape of valence molecular orbitals and in bonds of low polarity in which core contributions are negligible and the radial form of the valence orbitals dominates the total density[76,77]. The change in bond distance in the complexes from the PBE0/ECP(Ru,Cl)[6-31G*] to PBE0/ECP(Ru)[6-31+G(d,p)] optimized systems is less than 0.1 hatree and atomic properties obtained using a higher basis set DGDZVP(Ru)[6-31+G(d,p)] (Tables 8 and 9) and minimal basis set 3-21G are in a very closed proximities which is an indication that there is no serious change in the geometries of the systems when they were optimized with higher basis set (ECP(Ru)[6-31+G(d,p)]) and lower basis set (ECP(Ru,Cl) [6-31G*]), respectively. Another implication is that the all electron minimal basis set 3-21G is good enough for the construction of topological features of complexes especially when the system in big. However, the values of the Hamiltonian form of kinetic energy density (K) are under estimated using 3-21G basis set. The bond properties of the complexes obtained when the system was treated with ECP(Ru)[6-31+G(d,p)] are similar to that obtained from all electron basis set DGDZVP(Ru)[6-31+G(d,p)] (Table-8) but ECP is found to underestimate the atomic properties which is an indication that constructing the topological features with ECP may not accurately provide both intra and inter atomic properties of the complexes though provide the same trends of values.

The bond distances (GBL_I) computed for complex 1 at the two method of optimization (Table-8) are similar but there is a significant change in the dihedral angles of the carboxylic unit which resulted to one H-bonding in the system optimized with ECP(Ru,Cl)[6-31G*] but two when optimized with ECP(Ru)[6-31+G(d,p)]. The traceable reason is that the system optimized with ECP(Ru)[6-31+G(d,p)] is characterized with two relatively equal N-N-C=O dihedral angles of 61.61 and 62.37 while that of ECP(Ru,Cl)[6-31G*] have two different N-N-C=O dihedral angles of -124.77 and 2.37. The geometries located by the two method of optimization are local minimum with zero imaginary frequencies. In complex 2 there is single H-bonding when the topology was constructed with DGDZVP(Ru)[6-31+G(d,p)] (Fig. 3b, Table-8) or with ECP(Ru)[6-31+G(d,p)] but no HB was observed when 3-21G basis set was used for the system optimized with ECP(Ru,Cl)[6-31G*]. In the same complex, there is no noticeable change in the geometries obtained at two levels of optimization (the two hydrogen atoms are at a distance of 2.14 Å from each other) which is an indication that though 3-21G basis set can produce a similar result with the higher basis set but it may not completely give the detailed topological features of the complexes. The Laplacian plot of the electron density of complex 2 (Fig. 3b) shows that many of the atoms are on the same plane. The carbonyl oxygen of the carboxylic unit of the complexes as expected is highly electronegative that the oxygen of the hydroxyl unit but the Laplacian is lower and positive indicating the effect of non-covalent π-bond. In complex 3, there are also no traceable changes in the geometries and the topologies from both 3-21G and DGDZVP(Ru)[6-31+G(d,p)] (Table-8) and two H-bonding are recognized in both methods (Fig. 3c, Table-8).

All the ruthenium-ligand (Ru-L) bonds are characterized with positive $\nabla^2\rho(r)$ and a lesser values of $\rho(r)$ (within the range of 0.07 to 0.10) compare to the covalent bonds that exist within the atoms of each coordinated ligands (Table-8 and Fig. 3) which are characterized with negative $\nabla^2\rho(r)$ and higher $\rho(r)$ values (within the range of 0.2 to 0.41). This is an indication that the Ru-L bonds are non-covalent bonds like coordinate or ionic bonds and are weaker than the covalent bonds within the ligands. They are also characterized with higher values of ellipticity which have been pointed out to be a feature of a very flat electron density region that is usually characterized with a very low average values[78] for $\rho(r)$ and $\nabla^2\rho(r)$. The ellipticity is a quantity defined as $\varepsilon = (\lambda1/\lambda2 - 1)$; $\lambda1 \leq \lambda2 \leq \lambda3$ where $\lambda1$, $\lambda2$ and $\lambda3$ are the eigenvalues of the Hessian, measures the behaviour of the electron density at a given point, in the plane tangential to the interatomic surface. The ellipticity value ranges from zero to infinity and is widely regarded as a quantitative index of the π-character of the bond[79]. The Ru-L are also characterized with lower K and Lagrangian density (L), higher stretching (BPL-GBL_I), higher potentials (V is less negative) and lower magnitude of the ratio of potential and Lagrangian kinetic energy density (V/G). The very low average kinetic energy which is responsible for higher |V|/G has been pointed through the uncertainty principle to be the nature of loosely bound density[76].

The features of the metal-chloride bonds in complexes 1, 2 and 3 that contain coordinated chloride indicates that the chloride will be a good living group where necessary in their biological interactions which has been suggested to proceed through hydrolysis[41,69,80,81]. The Ru-Cl bonds are characterized with lowest $\rho(r)$ and $\nabla^2\rho(r)$ indicating that it is weaker than other Ru-L bonds but associate with lower stretching and lower ellipticity (Table-8). In these three complexes, the bond properties of the Ru-Cl are relatively the same which shows that the change in the chemical environment does not have serious effect on the M-Cl bond. Among all the ruthenium-ligand (Ru-L) bonds, the Ru-nitrogen bond (Ru-N) appears to be strongest with higher values of $\rho(r)$ and $\nabla^2\rho(r)$ and lowest stretching. The implication of this is that, in any possibility of the scissoring of complexes during biological interaction, the coordinated arene and chloride will be compromised for the bidentate and tridentate ligand. All the Ru-N bonds are also associated with

TABLE-8
SELECTED BOND PROPERTIES INVOLVING RUTHENIUM OR HYDROGEN BOND (BONDS WITH SUPERSCRIPT "#") OBTAINED THROUGH QTAIM ANALYSIS OF DGDZVP(Ru)[6-31+G(d,p)] BASIS SET TYPE OF SYSTEMS

Bonds	ρ(r)	$\nabla^2\rho(r)$	Ellipticity	K	BPL-GBL_I	V	G	L	GBL_I	V/G
Complex 1										
Ru1 - C10	0.077	0.235	0.621	0.015	1.50E-02	-0.088	0.073	-0.059	4.210	1.200
Ru1 - C13	0.077	0.231	0.658	0.015	1.84E-02	-0.088	0.073	-0.058	4.220	1.200
Ru1 - C19	0.078	0.237	1.030	0.015	1.99E-02	-0.089	0.074	-0.059	4.200	1.200
Ru1 - Cl22	0.073	0.216	0.162	0.011	1.06E-03	-0.075	0.065	-0.054	4.520	1.160
Ru1 - N17	0.082	0.415	0.428	0.005	1.88E-03	-0.114	0.109	-0.104	4.040	1.050
Ru1 - N12	0.082	0.417	0.417	0.005	2.00E-03	-0.114	0.109	-0.104	4.040	1.050
Complex 2										
Ru1 - C7	0.077	0.222	0.399	0.015	9.17E-03	-0.086	0.071	-0.056	4.220	1.220
Ru1 - C14	0.076	0.223	0.786	0.014	1.17E-02	-0.084	0.070	-0.056	4.230	1.200
Ru1 - C18	0.077	0.222	0.400	0.015	9.20E-03	-0.086	0.071	-0.056	4.220	1.220
Ru1 - Cl10	0.073	0.214	0.172	0.011	6.59E-04	-0.075	0.064	-0.053	4.530	1.170
Ru1 - N11	0.094	0.445	0.319	0.011	5.10E-03	-0.133	0.122	-0.111	3.960	1.090
Ru1 - N16	0.093	0.446	0.319	0.011	5.36E-03	-0.133	0.122	-0.111	3.960	1.090
Complex 3										
Ru1 - C13	0.074	0.248	1.930	0.012	5.19E-02	-0.086	0.074	-0.062	4.230	1.160
Ru1 - C14	0.072	0.240	1.600	0.011	3.01E-02	-0.083	0.071	-0.060	4.250	1.160
Ru1 - C18	0.074	0.246	1.800	0.012	4.85E-02	-0.086	0.074	-0.062	4.230	1.170
Ru1 - C23	0.072	0.241	2.010	0.011	3.73E-02	-0.082	0.071	-0.060	4.260	1.150
Ru1 - C21	0.071	0.241	2.940	0.011	8.17E-02	-0.081	0.071	-0.060	4.280	1.150
Ru1 - C25	0.071	0.238	2.000	0.011	5.91E-02	-0.082	0.070	-0.059	4.270	1.160
Ru1 - Cl7	0.073	0.222	0.195	0.011	7.90E-05	-0.077	0.066	-0.055	4.520	1.160
Ru1 - N10	0.083	0.418	0.434	0.006	3.61E-03	-0.116	0.110	-0.105	4.040	1.050
Ru1 - N16	0.082	0.418	0.439	0.006	3.50E-03	-0.116	0.110	-0.105	4.040	1.050
Complex 4										
Ru1 - C2	0.070	0.240	9.190	0.009	1.67E-01	-0.079	0.069	-0.060	4.280	1.130
Ru1 - C3	0.072	0.235	1.560	0.012	2.42E-02	-0.082	0.070	-0.059	4.260	1.170
Ru1 - C4	0.070	0.241	14.500	0.009	1.92E-01	-0.079	0.069	-0.060	4.280	1.130
Ru1 - C5	0.075	0.241	1.670	0.013	3.95E-02	-0.087	0.074	-0.060	4.240	1.180
Ru1 - C6	0.073	0.234	1.530	0.012	2.38E-02	-0.082	0.070	-0.059	4.260	1.170
Ru1 - C7	0.075	0.242	1.720	0.013	4.08E-02	-0.087	0.074	-0.060	4.240	1.180
Ru1 - N10	0.080	0.372	0.185	0.006	2.11E-02	-0.105	0.099	-0.093	4.090	1.060
Ru1 - N13	0.080	0.372	0.185	0.006	2.11E-02	-0.105	0.099	-0.093	4.090	1.060
Ru1 - N15	0.097	0.433	0.314	0.013	1.50E-02	-0.135	0.122	-0.108	3.940	1.110
Complex 5										
Ru1 - C18	0.073	0.238	1.790	0.012	4.69E-02	-0.084	0.072	-0.060	4.260	1.170
Ru1 - C20	0.070	0.227	1.520	0.011	2.19E-02	-0.078	0.068	-0.057	4.290	1.160
Ru1 - C22	0.073	0.238	1.720	0.013	4.50E-02	-0.084	0.072	-0.059	4.260	1.170
Ru1 - C26	0.070	0.228	1.550	0.011	2.23E-02	-0.078	0.068	-0.057	4.290	1.160
Ru1 - N14	0.084	0.372	0.146	0.008	1.83E-02	-0.109	0.101	-0.093	4.070	1.080
Ru1 - N15	0.109	0.469	0.285	0.021	9.59E-03	-0.158	0.138	-0.117	3.850	1.150
Ru1 - N21	0.084	0.371	0.144	0.008	1.83E-02	-0.109	0.101	-0.093	4.070	1.080

ρ(r) is electron density, $\nabla^2\rho$ is the Laplacian of ρ(r), BPL–GBL_I is bond strain, V is virial field (potential energy density), G is Lagrangian form of kinetic energy density, K is hamiltonian form of kinetic energy density, L (*i.e.*, K-G) is lagrangian density which is (-1/4) $\nabla^2\rho$ while "Ratio" is V/G *i.e.*, PE/KE (the higher its magnitude the stronger the bond)

higher K, V (less negative), G, L (less negative) but lower values of |V|/G compare to other Ru-L bonds. There is also no significant changes in the in the stretching of the Ru-arene and Ru-nitrogen (Ru-N) bonds (nitrogen from the bidentate and tridentate) in all the complexes except for the central pyridine unit of the tridentate that are characterized with stronger nature of coordinated bonds with metal (*i.e.*, higher values of ρ(r) and $\nabla^2\rho(r)$) than other Ru-N bonds.

The correlation of the bonds properties constructed over all the existing bonds in the complexes gives a clear picture of the factors that define a strong bond and their relationship. A strong bond with a high negative values of $\nabla^2\rho(r)$ (*i.e.*, covalent bond) or high positive values of $\nabla^2\rho(r)$ (*i.e.*, non-covalent bond) should also be characterized with high values of ρ(r). These strong bond should also be associated with lower ellipticity, lower bond length and bond stretching. The correlation of potential energy density (V) and the Lagrangian form of kinetic energy density (G) on the strength of bonds greatly become significant when considering their ratio (|V|/G). A stronger bond is characterized with high values of |V|/G, low Hamiltonian form of kinetic energy density (K) and highly negative values of Lagrangian density (L). The high correlation between V and G (-0.90, -0.90, -0.89, -0.84 and -0.88 respective complexes) indicates that the bonds with high V are usually associated with lower G. The values of K are highly correlated with the electron density (ρ(r)) of each atom (0.89, 0.88, 0.90, 0.90

TABLE-9
INTRA ATOMIC AND INTER ATOMIC PROPERTIES OF ATOMS INVOLVE IN METAL-LIGAND AND HYDROGEN BONDING (ATOMS WITH SUPERSCRIPT "#") OF SYSTEMS TREATED WITH DGDZVP(Ru)[6-31+G(d,p)] BASIS SET USING QTAIM ANALYSIS

	q(A)	L(A)	K(A)	K_Scaled(A)	Mu_Intra(A)	Mu_Bond(A)	|Mu(A)|	N(A)	LI(A)	%Loc(A)	DI(A,A')/2	%Deloc(A,A')	Vol(A),0.001
Complex 1													
Ru1	0.950	0.001	4440.000	-4450.000	0.126	1.140	1.200	43.100	40.500	94.100	2.540	5.900	101.000
C9	-0.063	0.000	37.800	-37.900	0.126	0.035	0.093	6.060	3.970	65.600	2.090	34.400	73.800
C10	-0.047	0.000	37.800	-37.900	0.089	0.080	0.061	6.050	3.960	65.500	2.090	34.500	71.400
C13	-0.050	0.000	37.800	-37.900	0.089	0.090	0.102	6.050	3.960	65.500	2.090	34.500	71.600
C16	-0.051	0.000	37.800	-37.900	0.134	0.099	0.055	6.050	3.970	65.600	2.080	34.400	73.700
C18	-0.058	0.000	37.800	-37.900	0.127	0.084	0.068	6.060	3.980	65.600	2.080	34.400	74.800
C19	-0.029	0.000	37.800	-37.900	0.118	0.136	0.102	6.030	3.950	65.500	2.080	34.500	69.900
Cl22	-0.527	0.000	459.000	-461.000	0.061	1.260	1.290	17.500	16.900	96.300	0.646	3.680	232.000
N12	-0.759	0.000	54.800	-54.900	0.695	0.810	0.658	7.760	5.900	76.100	1.860	23.900	78.100
N17	-0.759	0.000	54.800	-54.900	0.695	0.790	0.617	7.760	5.900	76.100	1.860	23.900	78.000
Complex 2													
Ru1	0.959	0.000	4440.000	-4450.000	0.085	1.120	1.180	43.000	40.500	94.000	2.570	5.960	104.000
C7	-0.053	0.000	37.800	-38.000	0.075	0.066	0.061	6.050	3.960	65.400	2.090	34.600	70.100
C8	-0.063	0.000	37.800	-37.900	0.137	0.079	0.082	6.060	3.980	65.600	2.080	34.400	74.600
C13	-0.053	0.000	37.800	-37.900	0.146	0.068	0.078	6.050	3.970	65.600	2.080	34.400	76.400
C14	-0.027	-0.001	37.800	-37.900	0.111	0.144	0.092	6.030	3.950	65.500	2.080	34.500	69.600
C18	-0.054	-0.001	37.800	-38.000	0.073	0.087	0.093	6.050	3.960	65.400	2.090	34.600	70.200
C19	-0.063	0.000	37.800	-37.900	0.137	0.066	0.074	6.060	3.980	65.600	2.080	34.400	74.600
Cl10	-0.521	0.000	459.000	-461.000	0.019	1.250	1.260	17.500	16.900	96.400	0.623	3.560	237.000
N11	-1.220	0.000	55.100	-55.200	0.223	0.743	0.542	8.220	6.360	77.400	1.860	22.600	82.100
N16	-1.220	0.000	55.100	-55.200	0.224	0.710	0.510	8.220	6.360	77.400	1.860	22.600	82.100
Complex 3													
Ru1	0.955	0.000	4440.000	-4450.000	0.090	0.833	0.840	43.000	40.500	94.100	2.520	5.860	99.900
C13	-0.040	0.000	37.800	-38.000	0.121	0.145	0.081	6.040	3.960	65.500	2.080	34.500	70.600
C14	-0.049	0.000	37.900	-38.000	0.121	0.281	0.400	6.050	3.970	65.600	2.080	34.400	69.800
C18	-0.040	0.000	37.800	-38.000	0.118	0.136	0.086	6.040	3.960	65.500	2.080	34.500	70.700
C21	-0.060	0.000	37.800	-38.000	0.099	0.102	0.132	6.060	3.970	65.500	2.090	34.500	73.600
C23	-0.050	0.000	37.900	-38.000	0.128	0.287	0.412	6.050	3.970	65.600	2.080	34.400	70.200
C25	-0.059	0.000	37.800	-38.000	0.096	0.113	0.140	6.060	3.970	65.500	2.090	34.500	73.300
Cl7	-0.533	0.000	459.000	-461.000	0.035	1.270	1.300	17.500	16.900	96.400	0.631	3.600	236.000
N10	-1.200	0.000	55.000	-55.200	0.200	1.140	0.947	8.200	6.360	77.500	1.840	22.500	83.000
N16	-1.200	0.000	55.000	-55.200	0.201	1.100	0.912	8.200	6.360	77.500	1.840	22.500	83.000
Complex 4													
Ru1	0.992	-0.001	4430.000	-4450.000	0.147	0.442	0.399	43.000	40.600	94.300	2.460	5.710	110.000
C2	-0.046	0.000	37.800	-37.900	0.132	0.071	0.066	6.050	3.970	65.600	2.080	34.400	73.300
C3	-0.044	0.000	37.800	-37.900	0.107	0.081	0.066	6.040	3.960	65.600	2.080	34.400	70.700
C4	-0.046	0.000	37.800	-37.900	0.133	0.087	0.092	6.050	3.970	65.600	2.080	34.400	73.400
C5	-0.034	0.000	37.800	-37.900	0.127	0.096	0.091	6.030	3.960	65.600	2.080	34.400	72.700
C6	-0.044	0.000	37.800	-37.900	0.106	0.088	0.081	6.040	3.960	65.600	2.080	34.400	70.600
C7	-0.034	0.000	37.800	-37.900	0.127	0.100	0.098	6.030	3.960	65.600	2.080	34.400	72.600
N10	-0.771	0.000	54.700	-54.900	0.728	0.796	0.594	7.770	5.950	76.600	1.820	23.400	82.900
N13	-0.771	0.000	54.700	-54.900	0.728	0.791	0.581	7.770	5.950	76.600	1.820	23.400	82.900
N15	-1.240	0.000	55.100	-55.300	0.186	0.447	0.331	8.240	6.400	77.700	1.840	22.300	80.600
Complex 5													
Ru1	0.982	0.001	4430.000	-4450.000	0.192	0.583	0.562	43.000	40.500	94.200	2.500	5.820	108.000
C18	-0.036	0.000	37.800	-37.900	0.126	0.082	0.056	6.040	3.960	65.600	2.080	34.400	72.600
C20	-0.048	0.000	37.800	-38.000	0.106	0.095	0.089	6.050	3.970	65.600	2.080	34.400	70.900
C22	-0.036	0.000	37.800	-37.900	0.127	0.085	0.063	6.040	3.960	65.600	2.080	34.400	72.600
C23	-0.049	0.000	37.800	-37.900	0.132	0.068	0.081	6.050	3.970	65.600	2.080	34.400	73.000
C26	-0.048	-0.001	37.800	-38.000	0.107	0.128	0.127	6.050	3.970	65.600	2.080	34.400	71.000
C27	-0.049	0.000	37.800	-37.900	0.131	0.091	0.107	6.050	3.970	65.600	2.080	34.400	72.900
N14	-1.230	0.000	55.000	-55.200	0.199	0.621	0.462	8.230	6.400	77.800	1.830	22.200	85.800
N15	-1.230	0.000	55.100	-55.300	0.216	0.369	0.232	8.230	6.350	77.200	1.880	22.800	79.000
N21	-1.230	0.000	55.000	-55.200	0.199	0.517	0.370	8.230	6.400	77.800	1.830	22.200	85.800

q(A) is net charge of atom A, L(A) is Lagrangian of Atom A, N(A) is average number of electrons in atom A, K(A) is electronic kinetic energy of atom A (Hamiltonian Form), % Loc(A) is percentage of average number of electrons localized in atom A, K_Scaled(A) is approximation to virial-based total energy of atom A, Mu_Intra (A) is magnitude of intraatomic dipole moment of atom A, Ee(A) is contribution of atom A to electronic energy of molecule, %Deloc(A,A') is the percentage of electron delocalization index of atom A and Vol(A) is the volume bounded by an isosurface of the electron density distribution (0.001) and by interatomic surfaces of atom A

and 0.88 respective complexes) and also have higher effect than G on the values of $\nabla^2\rho(r)$, ellipticity and bond distance.

Intra-atomic and inter-atomic properties: The properties of the atoms in each of the five complexes which are coordinated to metal are presented in the Table-9. The integrated Lagrangian values L(A) of all the atomic basins are approximately equals to zero, which is an indication of satisfactory numerical integration[76]. For all the atoms in the complexes

other than H atoms, the values of the percentage localization [% Loc(A)] are high while the percentage delocalization [% Deloc(A,A')]. The reverse nature of the % Loc(A) and % Deloc(A,A') of the H atoms indicates that they can be easily perturbed by an external electric field[76]. The hydrogen atoms that are involved in hydrogen bonds are characterized with higher charges, bonding dipole and total dipole than other hydrogen atoms in the complexes. Unlike what is observed in the ruthenium bond properties, the intra atomic and inter atomic properties of ruthenium atom in the complexes depends much on the chemical environment. The charges on the ruthenium atom in the tridentate complexes 4 and 5 are little higher than what is observed for the complexes 1, 2 and 3. Both the intra and bonding dipole of the metal vary significantly from one complex to the other and also its total dipole moment. The tridentate complexes 4 and 5 have higher intra atomic dipole for Ru atom but lower bonding dipole and total dipole than the three other complexes 1, 2 and 3 with coordinated chloride ligand. The charge distribution and intra atomic dipole moment of the coordinated chloride and nitrogen atoms of both bidentate and tridentate ligands change significantly also from one complex to the other. Other atomic properties of ruthenium atom like the number and the percentages of the localized or delocalized electrons and the volume of the electron density are not significantly varied in the complexes either with or without chloride ligand.

The correlation of the computed atomic properties gives the summary of the changes in the properties in relation to each other. The atoms that are highly electronegative in the complexes are associated with higher bonding dipole, total dipole and higher volume of atomic density. The high number of electrons or of localized electron significantly favours the bonding dipole, total dipole and volume of electron density of the complexes while high de-localization has reverse effects. The total dipole of each atom is significantly determined by its bonding dipole than the contribution of its intra atomic dipole.

Conclusion

The electronic and structural properties of the complexes 1, 2, 3, 4 and 5 have been computed using the hybrid function B3LYP of the system optimized at PBE0 level of theories. The geometries of the complexes have been found to be thermodynamically stable. Optimisation of the complexes at lower basis set ECP(Ru,Cl)[6-31+G*] and higher basis set ECP(Ru)[6-31+G(d,p)] does not significantly affect the bond distances of the complexes but a significant change in the dihedral angles of complexes 1 was observed which resulted to differences in the number of hydrogen bonds. The obtained values of energy using different functional and basis sets ranging from 3-21G to aug-cc-pVTZ shows that the energy of these complexes are significantly affected by the choice of the functional than the choice of basis sets. The stability of these complexes is significantly enhanced through the high level of charge transfer (CT), polarizability (POL) and electrostatic (ES) contributions. The presence of the carboxylic unit is found to significantly enhance the stability of these complexes which may contribute to their biological activity as anticancer agent. All the ruthenium-ligand (Ru-L) bonds are found to be non-covalent in nature and the Ru-N bonds are shown to be strongest among all the Ru-L bonds. The contraction and the consequential stronger Ru-N bonds of the $Ru\text{-}N_{bpyr}$ in complex 2 compare to $Ru\text{-}N_{phn}$ bond in complex 3 agrees with the experimental report. The QTAIM analysis shows that Ru-Cl is weaker than every other metal-ligand bonds which is expected for the activation to take place by hydrolysis but the bond order gives a contrary view. The characteristic features of the charge transfer are very complicated which resulted to the metal atom and the chloride ligand (where applicable) being characterized as part of both HOMO and the LUMO. The study shows that there is significant electron lose from the ruthenium orbitals in coordinating with the ligands (ruthenium atom predominantly the HOMO) but there is high charge transfer (back bonding of electrons) from the ligand orbitals into the lower energy vacant anti-bonding lone pair orbitals of the ruthenium atom which is being responsible for the LUMO contribution of the metal centre. The strength of the Ru-N bonds in the complexes follows the order 5 > 2 > 4 > 3 > 1 if only the mid Ru-N bond is considered.

ACKNOWLEDGEMENTS

The authors gratefully acknowledge the financial support of Govan Mbeki Research and Development Centre, University of Fort Hare, South Africa. The CHPC and CSIR, Department of Science and Technology, Republic of South Africa are gratefully acknowledge for providing the computing facilities and some software's that are used for the computation.

REFERENCES

1. C.S. Allardyce, A. Dorcier, C. Scolaro and P.J. Dyson, *Appl. Organomet. Chem.*, **19**, 1 (2005).
2. P.J. Dyson and G. Sava, *J. Chem. Soc., Dalton Trans.*, **23**, 1929 (2006).
3. P. Heffeter, K. Böck, B. Atil, M.A. Reza Hoda, W. Körner, C. Bartel, U. Jungwirth, B.K. Keppler, M. Micksche, W. Berger and G. Koellensperger, *J. Biol. Inorg. Chem.*, **15**, 737 (2010).
4. G. Zhao and H. Lin, *Curr. Med. Chem.*, **5**, 137 (2005).
5. M. Bacac, A.C.G. Hotze, K. Schilden, J.G. Haasnoot, S. Pacor, E. Alessio, G. Sava and J. Reedijk, *J. Inorg. Biochem.*, **98**, 402 (2004).
6. A.H. Velders, A. Bergamo, E. Alessio, E. Zangrando, J.G. Haasnoot, C. Casarsa, M. Cocchietto, S. Zorzet and G. Sava, *J. Med. Chem.*, **47**, 1110 (2004).
7. A.V. Vargiu, A. Robertazzi, A. Magistrato, P. Ruggerone and P. Carloni, *J. Phys. Chem. B*, **112**, 4401 (2008).
8. P. Mura, M. Camalli, L. Messori, F. Piccioli, P. Zanello and M. Corsini, *Inorg. Chem.*, **43**, 3863 (2004).
9. A.A. Hostetter, M.L. Miranda, V.J. DeRose and K.L. McFarlane Holman, *J. Biol. Inorg. Chem.*, **16**, 1177 (2011).
10. A. Bergamo, B. Gava, E. Alessio, G. Mestroni, B. Serli, M. Cocchietto, S. Zorzet and G. Sava, *Int. J. Oncol.*, **21**, 1331 (2002).
11. B.S.P. Enzo Alessio, B.S.P. Giovanni Mestroni, B.S.P. Alberta Bergamo and B.S.P. Gianni Sava, *Curr. Top. Med. Chem.*, **4**, 1525 (2004).
12. A. Bergamo, C. Gaiddon, J.H. Schellens, J.H. Beijnen and G. Sava, *J. Inorg. Biochem.*, **106**, 90 (2012).
13. I. Bratsos, D. Urankar, E. Zangrando, P. Genova-Kalou, J. Košmrlj, E. Alessio and I. Turel, *Dalton Trans.*, **40**, 5188 (2011).
14. M. Brindell, E. Kulis, S.K. Elmroth, K. Urbanska and G. Stochel, *J. Med. Chem.*, **48**, 7298 (2005).
15. E. Cabrera, H. Cerecetto, M. González, D. Gambino, P. Noblia, L. Otero, B. Parajón-Costa, A. Anzellotti, R. Sánchez-Delgado, A. Azqueta, A.L. de Ceráin and A. Monge, *Eur. J. Med. Chem.*, **39**, 377 (2004).
16. K.D. Camm, A. El-Sokkary, A.L. Gott, P.G. Stockley, T. Belyaeva and P.C. McGowan, *Dalton Trans.*, 10914 (2009).
17. M. Hirano, Y. Sakate, H. Inoue, Y. Arai, N. Komine, S. Komiya, X. Wang and M.A. Bennett, *J. Organomet. Chem.*, **708-709**, 46 (2012).

18. M.A. Bennett, M.J. Byrnes, G. Chung, A.J. Edwards and A.C. Willis, *Inorg. Chim. Acta*, **358**, 1692 (2005).
19. P. Pertici, A. Verrazzani, G. Vitulli, R. Baldwin and M.A. Bennett, *J. Organomet. Chem*., **551**, 37 (1998).
20. M.A. Bennett, A.J. Edwards, J.R. Harper, T. Khimyak and A.C. Willis, *J. Organomet. Chem*., **629**, 7 (2001).
21. M.A. Bennett, A.M. Clark, M. Contel, C.E.F. Rickard, W.R. Roper and L.J. Wright, *J. Organomet. Chem*., **601**, 299 (2000).
22. M.A. Bennett, *Coord. Chem. Rev*., **166**, 225 (1997).
23. M.A. Bennett, M. Bown and M.J. Byrnes, *J. Organomet. Chem*., **571**, 139 (1998).
24. M.A. Bennett, Comprehensive Organometallic Chemistry II, vol. 7, p. 441 (1995).
25. V. Vajpayee, Y.J. Yang, S.C. Kang, H. Kim, I.S. Kim, M. Wang, P.J. Stang and K.W. Chi, *Chem. Commun.*, **47**, 5184 (2011).
26. F. Schmitt, P. Govindaswamy, O. Zava, G. Süss-Fink, L. Juillerat-Jeanneret and B. Therrien, *J. Biol. Inorg. Chem*., **14**, 101 (2009).
27. G. Süss-Fink, *Dalton Trans*., **39**, 1673 (2010).
28. J. Ruiz, C. Vicente, C. de Haro and D. Bautista, *Dalton Trans*., 5071 (2009).
29. A. Martínez, J. Suárez, T. Shand, R.S. Magliozzo and R.A. Sánchez-Delgado, *J. Inorg. Biochem*., **105**, 39 (2011).
30. C. Gossens, I. Tavernelli and U. Rothlisberger, *J. Am. Chem. Soc*., **130**, 10921 (2008).
31. F. Barragán, P. López-Senín, L. Salassa, S. Betanzos-Lara, A. Habtemariam, V. Moreno, P.J. Sadler and V. Marchán, *J. Am. Chem. Soc*., **133**, 14098 (2011).
32. T. Bugarcic, A. Habtemariam, J. Stepankova, P. Heringova, J. Kasparkova, R.J. Deeth, R.D. Johnstone, A. Prescimone, A. Parkin, S. Parsons, V. Brabec and P.J. Sadler, *Inorg. Chem*., **47**, 11470 (2008).
33. M. Castellano-Castillo, H. Kostrhunova, V. Marini, J. Kasparkova, P.J. Sadler, J.M. Malinge and V. Brabec, *J. Biol. Inorg. Chem*., **13**, 993 (2008).
34. J. Dougan, A. Habtemariam, S.E. McHale, S. Parsons and P.J. Sadler, *Proc. Natl. Acad. Sci. USA*, **105**, 11628 (2008).
35. S.J. Dougan, M. Melchart, A. Habtemariam, S. Parsons and P.J. Sadler, *Inorg. Chem*., **45**, 10882 (2006).
36. R. Fernández, M. Melchart, A. Habtemariam, S. Parsons and P.J. Sadler, *Chem. Eur. J*., **10**, 5173 (2004).
37. Y. Fu, A. Habtemariam, A.M. Basri, D. Braddick, G.J. Clarkson and P.J. Sadler, *Dalton Trans*., **40**, 10553 (2011).
38. A. Casini, C. Gabbiani, F. Sorrentino, M.P. Rigobello, A. Bindoli, T.J. Geldbach, A. Marrone, N. Re, C.G. Hartinger, P.J. Dyson and L. Messori, *J. Med. Chem*., **51**, 6773 (2008).
39. S. Chatterjee, S. Kundu, A. Bhattacharyya, C.G. Hartinger and P.J. Dyson, *J. Biol. Inorg. Chem*., **13**, 1149 (2008).
40. M. Groessl, Y.O. Tsybin, C.G. Hartinger, B.K. Keppler and P.J. Dyson, *J. Biol. Inorg. Chem*., **15**, 677 (2010).
41. A.E. Egger, C.G. Hartinger, A.K. Renfrew and P.J. Dyson, *J. Biol. Inorg. Chem*., **15**, 919 (2010).
42. W.H. Ang, E. Daldini, C. Scolaro, R. Scopelliti, L. Juillerat-Jeannerat and P.J. Dyson, *Inorg. Chem*., **45**, 9006 (2006).
43. C.A. Vock, W.H. Ang, C. Scolaro, A.D. Phillips, L. Lagopoulos, L. Juillerat-Jeanneret, G. Sava, R. Scopelliti and P.J. Dyson, *J. Med. Chem*., **50**, 2166 (2007).
44. W.H. Ang, E. Daldini, L. Juillerat-Jeanneret and P.J. Dyson, *Inorg. Chem*., **46**, 9048 (2007).
45. W.H. Ang, A. De Luca, C. Chapuis-Bernasconi, L. Juillerat-Jeanneret, M. Lo Bello and P.J. Dyson, *Chem. Med. Chem*., **2**, 1799 (2007).
46. N.P. Barry, O. Zava, P.J. Dyson and B. Therrien, *Chem. Eur. J*., **17**, 9669 (2011).
47. N.P. Barry, O. Zava, J. Furrer, P.J. Dyson and B. Therrien, *Dalton Trans*., **39**, 5272 (2010).
48. A.A. Adeniyi and P.A. Ajibade, *J. Mol. Graph. Model*., **38**, 60 (2012).
49. I. Alkorta, F. Blanco, J. Elguero, J.A. Dobado, S.M. Ferrer and I. Vidal, *J. Phys. Chem. A*, **113**, 8387 (2009).
50. A. Hinchlinffe, Chemical Modelling: Applications and Theory, the Royal Society of Chemistry, Thomas Graham House, Science Park, Milton Road, Cambridge CB4 0WF, UK, Vol. 5, pp. 13-15 (2008).
51. C. Adamo and V. Barone, *J. Chem. Phys*., **110**, 6158 (1999).
52. W.J. Stevens, M. Krauss, H. Basch and P.G. Jasien, *Can. J. Chem*., **70**, 612 (1992).
53. D.J. Feller, *Comput. Chem*., **17**, 1571 (1996).
54. K.L. Schuchardt, B.T. Didier, T. Elsethagen, L. Sun, V. Gurumoorthi, J. Chase, J. Li and T.L. Windus, *J. Chem. Inf. Model*., **47**, 1045 (2007).
55. A.A. Granovsky, Firefly version 8.0.G, www http://classic.chem.msu.su/gran/firefly/index.html (2013).
56. M.J. Frisch, G.W. Trucks, H.B. Schlegel, G.E. Scuseria, M.A. Robb, J.R. Cheeseman, G. Scalmani, V. Barone, B. Mennucci, G.A. Petersson, H. Nakatsuji, M. Caricato, X. Li, H.P. Hratchian, A.F. Izmaylov, J. Bloino, G. Zheng, J.L. Sonnenberg, M. Hada, M. Ehara, K. Toyota, R. Fukuda, J. Hasegawa, M. Ishida, T. Nakajima, Y. Honda, O. Kitao, H. Nakai, T. Vreven, J.A. Montgomery Jr., J.E. Peralta, F. Ogliaro, M. Bearpark, J.J. Heyd, E. Brothers, K.N. Kudin, V.N. Staroverov, R. Kobayashi, J. Normand, K. Raghavachari, A. Rendell, J.C. Burant, S.S. Iyengar, J. Tomasi, M. Cossi, N. Rega, J.M. Millam, M. Klene, J.E. Knox, J.B. Cross, V. Bakken, C. Adamo, J. Jaramillo, R. Gomperts, R.E. Stratmann, O. Yazyev, A.J. Austin, R. Cammi, C. Pomelli, J.W. Ochterski, R.L. Martin, K. Morokuma, V.G. Zakrzewski, G.A. Voth, P. Salvador, J.J. Dannenberg, S. Dapprich, A.D. Daniels, O. Farkas, J.B. Foresman, J.V. Ortiz, J. Cioslowski and D.J. Fox, Gaussian, Inc., Wallingford CT (2009).
57. B. Marchal, P. Carbonniére, D. Begue and C. Pouchan, *Chem. Phys. Lett*., **453**, 49 (2008).
58. R. Marchal, P. Carbonnière and C. Pouchan, *Comput. Theoret. Chem*., **990**, 100 (2012).
59. A. Bagno and M. Bonchio, *Eur. J. Inorg. Chem*., 1475 (2002).
60. A.D. Becke, *J. Chem. Phys*., **98**, 5648 (1993).
61. K.D. Dobbs and W.J. Hehre, *J. Comput. Chem*., **8**, 861 (1987).
62. T.A. Keith, AIMAll (Version 12.06.03), TK Gristmill Software, Overland Park KS, USA (2012).
63. A.E. Reed, L.A. Curtiss and F. Weinhold, *Chem. Rev*., **88**, 899 (1988).
64. J.P. Foster and F.J. Weinhold, *J. Am. Chem. Soc*., **102**, 7211 (1980).
65. E.D. Glendening and A.J. Streitwieser, *Chem. Phys*., **100**, 2900 (1994).
66. V. Tognetti and L. Joubert, *J. Phys. Chem. A*, **115**, 5505 (2011).
67. P. Uma Maheswari, V. Rajendiran, M. Palaniandavar, R. Thomas and G.U. Kulkarni, *Inorg. Chim. Acta*, **359**, 4601 (2006).
68. A.K. Renfrew, A.D. Phillips, E. Tapavicza, R. Scopelliti, U. Rothlisberger and P.J. Dyson, Organometallics, **28**, 5061 (2009).
69. G. Gasser, I. Ott and N. Metzler-Nolte, *J. Med. Chem*., **54**, 3 (2011).
70. M. Hanif, H. Henke, S.M. Meier, S. Martic, M. Labib, W. Kandioller, M.A. Jakupec, V.B. Arion, H. Kraatz, B.K. Keppler and C.G. Hartinger, *Inorg. Chem*., **49**, 7953 (2010).
71. R. Parthasarathi and V. Subramanian, Characterization of Hydrogen Bonding: From van der Waals Interactions to Covalency; In: Hydrogen Bonding–New Insights, Springer, Vol. 3, Chap.1, pp. 1–50 (2006).
72. S.J. Grabowski, W.A. Sokalski and J. Leszczynski, *Chem. Phys. Lett*., **432**, 33 (2006).
73. I. Alkorta, J. Elguero and J.E. Del Bene, *Chem. Phys. Lett*., **489**, 159 (2010).
74. U. Koch and P.L. Popelier, *J. Phys. Chem*., **99**, 9747 (1995).
75. Q.K. Timerghazin, I. Rizvi and G.H. Peslherbe, *J. Phys. Chem. A*, **115**, 13201 (2011).
76. J.A. Platts, J. Overgaard, C. Jones, B.B. Iversen and A. Stasch, *J. Phys. Chem. A*, **115**, 194 (2011).
77. K.E. Edgecombe, R.O. Esquivel, V.H. Smith and F. Müller-Plathe, *J. Chem. Phys*., **97**, 2593 (1992).
78. L.J. Farrugia and H.M. Senn, *J. Phys. Chem. A*, **116**, 738 (2012).
79. G. Gopakumar, V.T. Ngan, P. Lievens and M.T. Nguyen, *J. Phys. Chem. A*, **112**, 12187 (2008).
80. M. Hanif, H. Henke, S.M. Meier, S. Martic, M. Labib, W. Kandioller, M.A. Jakupec, V.B. Arion, H. Kraatz, B.K. Keppler and C.G. Hartinger, *Inorg. Chem*., **49**, 7953 (2010).
81. F. Wang, A. Habtemariam, E.P.L. van der Geer, R. Fernandez, M. Melchart, R.J. Deeth, R. Aird, S. Guichard, F.P.A.P. Fabbiani, I.D.H. Lozano-Casal, I.D.H. Oswald, D.I. Jodrell, S. Parsons and P.J. Sadler, *Proc. Natl. Acad. Sci. USA*, **102**, 18269 (2005).